

# Explicating the role of scale-dependent processes in landscape transition & stability

A.K. Naylor, G.S. Okin, P. D'Odorico

July 30, 2020

## Abstract

While self-organization is often invoked in landscape change, particularly heterogeneous landscapes exhibiting multiple states, the role of scale and interpretation of vegetation heterogeneity and distributions, in particular the application of power laws to vegetation cluster distributions, remains vague. We explicitly test the role of feedback scale and feedback strength in driving self-organization of heterogeneous landscapes using a kernel-based model and a robust, nonparametric test for power-law probability, as well as performance under both continuous and event-based stress. We find three distinct stable states: one without power-law structure, one with uniform power law structure across the entire landscape, and third stable state with heterogeneous power law structure exhibited in disconnected clusters, supporting the hypothesis that such heterogeneous landscapes represent a true alternative state. Landscape resilience under consistent stress and recovery after a landscape-wide mortality event is also dependent on scale of feedback processes. Landscape-scale connectivity is broken by stress at both large scales. Less extensive feedbacks are less affected, allowing them to serve as nuclei for landscape-wide recovery. Better understanding of different morphologies can help constrain the still-unclear processes leading to the development of heterogeneity in landscapes, and insights from the breaking of feedback contiguity provide insights into landscape response to disturbance and potential for recovery.

## 1 Introduction

Landscapes can be described as linked systems of biological, climatic, geochemical and geomorphic processes that have preferred equilibria, i.e. landscapes tend to exist in relatively discrete states characterized by a dominant surface cover (*Holling*, 1973; *Noy-Meir*, 1975; *Westoby et al.*, 1989). On coarse spatial scales this means that over some spatio-temporal gradient—such as temperature, nutrient supply, or moisture—there are associated transitions in landscape systems. This dynamic is most strongly associated with the boundaries of woody ecosystems, particularly the expansion of desert shrubs (“desertification”) but also the tundra-taiga boundary, alpine treelines, tropical forest-grassland boundaries, and mangrove expansion.

On a *landscape scale* these can systems be considered bistable, with landscape states shift past a threshold or, if there are intra-landscape negative feedback process, hysteresis that prevents such a shift. The definition of these internal feedback effects is poorly understood, as is its relation with what can be termed *local-scale* bistability, such as the size distribution and topology of vegetation patches and gaps independent of topographical influences (*Lejeune et al.*, 1999; *Rietkerk et al.*, 2004). This dynamic

is most strongly associated with the boundaries of woody ecosystems, particularly the expansion of desert shrubs (“desertification”) but also the tundra-taiga boundary, alpine treelines, tropical forest-grassland boundaries, and mangrove expansion. While hysteresis effects can be explicitly invoked to explain local instability (e.g. *Yizhaq et al.* 2007 in the case of mixed vegetated and bare dunefields), the exact process basis for such facilitative feedbacks is not entirely clear (*Stewart et al.*, 2014). Potential facilitative feedbacks include some combination root-zone hydraulic feedbacks, under-canopy effects such as the capture of longwave radiation (reducing freezing risk at night), shading (reducing heat stress in the day) and nutrient capture (*D’Odorico et al.*, 2013a,b; *Runyan et al.*, 2012; *Wang et al.*, 2012). Additionally, the question of these local-scale processes may add up to an overall landscape shift—or whether landscape- and local-scale shifts should be considered separate, allometric processes—is generally elided.

To connect local heterogeneity with overall landscape change, power-law relationships ( $\Pr(A \geq a) \propto a^{-\alpha}$ , where  $a$  is some minimum patch or cluster size,  $A$  some larger cluster size, and  $\alpha$  the slope of the relationship in log-log space) are often invoked, since this pattern of scale invariance is typical of a classical phase transition. In cases of self-organized criticality such power-law relationships can occur in response to disturbance without a system-wide catastrophic shift in state; scaling behavior arises from the relationship between elements in the system, in ecological cases spatially connected feedbacks (*Bak et al.*, 1987; *Solé and Manrubia*, 1995). While earlier studies therefore suggested power law relationships among patch sizes may be indicative of landscape state change (*Rietkerk et al.*, 2004), *Pascual and Guichard* (2005) suggested the term “robust criticality” to describe systems that exhibit power-law scaling in a very broad parameter space without evidence of threshold behavior. Robust criticality has the potential to explain potentially very long-lived heterogeneous landscapes, with *Scanlon et al.* (2007) and *Moreno-de las Heras et al.* (2011) finding evidence of robustly critical scaling in savannas and mulga shrublands, respectively. The persistence of such landscapes over long terms raises the possibility that such states are not transitional, but either metastable or a while third states in themselves (*Okin et al.*, 2009; *Pascual and Guichard*, 2005; *Sankaran et al.*, 2004). The relationship between scale invariance and remains empirically ambiguous, with differing studies showing differing results, including areas of local-scale heterogeneity and evident of transition without without scale invariance *Kéfi et al.* (2007); *Maestre and Escudero* (2009); *Moreno-de las Heras et al.* (2011). The applicability of such power-law relationships has come into questions in studies of social, transport, computational, and metabolic networks, so a similar investigation of power law applicability in ecogeography is in order.

To untangle the scaling relationships between local- and landscape-level changes we explicitly test how different scales ( $\sigma$ ) of a simple model of spatial interaction operate at different feedback strengths ( $\phi$ ) under different levels of aspatial establishment-mortality ratios ( $M$ ) and external variability ( $\beta$ ); this provides a proxy for increasing interannual change of a landscape, as resources such as rain or limits such as cold become more variable either under some climatic change or across some spatial variant where a resource such as water or temperature becomes more variable (D'Odorico *et al.*, 2013a). For weak feedback processes, we would expect changes to show a greater signature of the either initial state or aspatial influences, with weak feedbacks operating at wide spatial scales acting to homogenize landscapes, albeit with few signs of structure expressed by power law distributions. In contrast, we would expect self-organizing dynamics from stronger feedbacks, with either local, structured heterogeneity at low feedback extents and strong threshold landscape-wide behavior for strong feedbacks acting on large spatial scales (figure 1). For strong feedbacks at narrow spatial scales, we expect local scale bistability, while at weak feedbacks at extensive scale large-scale heterogeneity is expected.

Early models of landscape heterogeneity, such as (Katori *et al.*, 1998)'s Ising-based model of tropical rainforest canopy gaps caused by trees felled by wind, relied on direct adjacency of cells. Hydrologically-based models, initially geared towards the study of banded vegetation on hillslopes (Lefever and Lejeune, 1997), used Gaussian kernel-based models to model longer-range hydrological processes; such models include not only short-range facilitation within vegetation patches but long-range competition between them. While this method does effectively simulate landscape patterns, it has been criticized for having a weak basis in process (Stewart *et al.*, 2014). Additionally, it is less clear whether facilitation-competition models effectively scale up to landscape-level changes; the feedbacks commonly invoked in large-scale landscape change are largely facilitative. D'Odorico *et al.* (2006)'s model is based on a facilitation-competition kernel based on the subtraction of two Gaussians, but results in a stable landscapes based on local feedbacks and the strength of spatial feedback, not its spatial scale. Rietkerk *et al.* (2004) makes an argument for the combined effects of feedback strength and feedback *scale* based on a changing the size and values of a convolution matrix, but this is more an illustrative example for different patch or gap sizes and topologies than a continuous model of landscape change, not an actual model of landscape dynamics in response to outside forcings.

## 2 Model description

State is defined by a binary variable  $s = 0, 1$  on the two-dimensional state grid  $S$  (here  $1000 \times 1000$  cells with periodic boundary conditions; cover of  $s = 1$  is designated  $c$ . For simplicity we describe 0 as bare and 1 as vegetated, but they could just as easily be reversed or describe two different kinds of vegetation (e.g. grass and shrub). The maintenance or change of state at each gridcell as a function of time  $s(t)$  is determined by two processes: aspatial stochastic state changes and state changes governed by spatially-dependent interactions among cells. Other potential factors, modeling such qualities as maturity or biomass, are ignored. While this does not produce a model with a close *biological* analogue to the processes outlined in section 1, it does provide guideposts for future identification of spatially-dependent facilitative interactions, which also tend to exhibit a pattern of rapid initial growth with long persistence modeled here, especially in such cases noted above as shrub encroachment (*Götmark et al., 2016*).

We initialize each individual cell on  $S_{(x,t=0)} = 1$  base on the starting proportion  $c_0$ , randomly distributed across based on ten random seeds to e sure no one starting condition biases results. The probability that some site  $x$  on  $S$  at timestep  $t$  will be of either state is governed by:

$$\Pr(S_{x=1, t}) = \Pr(E_x) - M \Pr(E_x) + V_{x, t-1}(U_{x, t-1}, S_{x, t-1}) \quad (1)$$

The first and second terms in the equation represent aspatial, randomly-distributed establishment and mortality, with the ratio between establishment and mortality given by  $M$ .  $\Pr(E_x)$  is given by

$$\Pr(E_x) = C_E 10^{\log_{10} \beta - 0.5 \log_{10} M} \quad (2)$$

where  $\beta$  is a parameter controlling the amount of *aspatial* (or external) variability in the landscape from timestep to timestep (analogous to [inverse] temperature in an Ising model, or in a geo-ecological context landscape-wide climate variability) and  $C_E$  is a scaling constant to translate from  $\Pr(E_x)$  of any individual cell to fractions of the entire landscape area. Mortality parameter  $M$  is used in calculating the establishment rate as well, since an environment with high mortality of for vegetated cells will likewise not have favorable conditions for expansion to new sites, even if there is high potential for “churn” in the landscape. This approach allows for us to test constant ratios of random establishment to random mortality even as  $\beta$  increases. We test three cases: an steady-state case where  $M = 1$  [ $\Pr(E_x)/M \Pr(E_x) = 1$ ], a rising establishment condition where  $M = 0.4$  [ $\Pr(E_x)/M \Pr(E_x) = 2.5$ ] and a declining establishment condition where  $M = 2$  [ $\Pr(E_x)/M \Pr(E_x) = 0.5$ ].

The third term in *eq. 1*, probability of *spatially-dependent* establishment and mortality (our internal dynamics), is defined by the spatial interaction grid  $U$ , a two-dimensional Gaussian blur of the initial state grid controlled by the standard deviation  $\sigma \in [1, 4]$  at intervals of 0.5, controlling the degree of spatial interaction. We only use one Gaussian to model spatial interaction, unlike other models such as *D'Odorico et al.* (2006) that use the difference of two Gaussian functions to model facilitation-competition over space models with discrete areas of facilitation-competition *Rietkerk et al.* 2004. Since the blur is extended over both states we are focusing on “vegetated” cells, we only need consider cases where  $c_0 \leq 0.5$ , since  $c_0 \geq 0.5$  would produce the symmetric results with “gaps.”

The importance of local facilitation in determining the state of each cell relative to its state in the previous timestep  $t - 1$  is controlled by a feedback parameter  $\phi$  (figure 2). A new grid of potential values at sites,  $V$ , is thus calculated as

$$V_{x, t-1} = \phi U_{x, t-1} + (1 - \phi) S_{x, t-1} \quad (3)$$

Values on sites  $V_{x, t-1}$  form a continuous range (0, 1) representing the probability for an individual site to be occupied by a woody plant in timestep, and drawing from these probabilities to arrive at values of 0 and 1 produces  $S_{x, t}$ . To ensure greater model stability from timestep to timestep (reflecting conditions in nature, where dramatic fluctuations in woody plant populations from year-to-year are rare), after the initial calculation of  $U$  values of less than 0.02 are set to 0 and more than 0.98 set to 1 to guarantee they remain bare or vegetated.

Model runs are performed for 1000 timesteps, with results presenting at 500 timesteps (depending on the species of cover analogized, each timestep could represent anything from a growing season to a few decades). The 500 timesteps are sufficient for a spin-up for the majority of each landscape to arrive at final state while allowing for the display of some transitional areas; 1000 timestep runs were made to check the persistence of intermediate states. When testing for hysteresis after a mortality event,  $M$  is increased to a 8 for the time interval  $t = [300, 399]$ , with the assumption  $\beta$  remains constant over the entire model run, i.e. an environment with more background variability will also experience a more destructive mortality event.

Clusters are identified using a Hoshen-Kopelman algorithm using von Neumann neighborhoods and all grids have toroidal boundary conditions. For determining the presence of power law distributions, our approximate proxy for critical landscape structure, we only take cases with fifty or greater power different cluster sizes and, using the powerlaw module developed by *Alstott et al.* (2014), performed

maximum likelihood estimates for every potential value of minimum cluster size  $a$  (eq. 1), choosing the values for  $a$  and  $\alpha$  that minimize the Kolmogorov-Smirnov statistics  $D$ , corresponding to the distance between the data and fit. We use the in nonparametric test for long-tailed distributions in *Clauset et al.* 2009; *Virkar and Clauset* 2014; *Vuong* 1989), where a  $p$ -value is calculated by bootstrapping the distribution, generating synthetic datasets to compare to the original model to arrive at a set of bootstrapped  $D_b$ -values. By comparing the ratios to test the likelihood that we have a scale-free distribution, with one being more likely. To give a precision  $\epsilon$  of one decimal digit we generate twenty-five synthetic datasets in accordance with the rule-of-thumb that the number of datasets should equal  $(\epsilon/4)^{-2}$ . Any values where  $p \leq 0.1$  are rejected, though such low values would only represent weak support for a power law so  $p$ -values should be interpreted as rough levels of support rather than a definitive test.

### 3 Model Results

Results displaying cover and power law probability—our proxy for structure—are depicted in figure 3. Rows 3a and 3b describe cases where the starting cover  $c_0 = 0.35$  and  $\beta = 1$  and  $\beta = 5$ , respectively. 3c describes where  $c_0 = 0.5$  and  $\beta = 1$  (increasing  $\beta$  at  $c_0 = 0.5$  has little effect on cover and similar effects on pattern as in 3b). Columns correspond to mortality ratio  $M$ , so when individual charts from figure 3 are referred to we add this to the figure number (e.g. figure 3b-0.4). Figure 4 displays the spatial distribution of vegetated cells at  $t = 500$  for the case of  $M = 1$  (even establishment and mortality), with lettering following the same  $(c_0, \beta)$  parameters as in figure 3, with areas on the  $(\sigma, \phi)$  denoted by i. (low state, minimal  $(\sigma, \phi)$ ), ii. (intermediate state, minimal  $\sigma$ , maximal  $\phi$ ), iii. (transition between states, medium  $(\sigma, \phi)$ ), and iv. (“high” state, maximal  $(\sigma, \phi)$ ). This convention holds through figures 5 and 6, discussing response of the system after disturbance. Similarly, figure 5 shows  $(c_{50}, \sigma, \phi)$  results after a mortality event ( $M$  increased to 8) occurs in the time interval  $t = [300, 399]$  and figure 6 corresponding cover maps. Note that these are mapped in parameter spaces, not space or time, with  $\sigma$  and  $\phi$  staying constant for each run. We mainly report results for  $M \in [0.4, 2]$  since for the former there is universal growth without structure and the latter universal mortality without structure.  $c_0 = 0.2$  largely follows the same pattern as  $c_0 = 0.35$  albeit at lower coverage, and  $c_0 > 0.5$  is symmetrical but with vegetated and gap areas reversed. Additionally there is a special case at where cover is the same across the entire parameter space, allowing for a control case for different morphologies of cluster and gap distribution.

Across all cases in figure 3 we can identify either a low state or an advanced transition to one. At low noise the smaller initial starting populations are overwhelmed by the initial higher levels of

cover. Even in this high-establishment case in 3a-0.4, small, localized feedbacks are *still* sufficient to drive overall land cover down, as larger initial local gaps prevent new establishment and reinforce new mortality, resulting shrinking vegetated space even when overall establishment rates are high. In figure 4a-i (under steady-state establishment and mortality  $M = 1$ ) we see the effect of these dynamics: apart from the small amount of snow from interannual noise, cover is in a few where vegetation only remains in clusters of sufficient size to allow resilience, leading to a cluster size distribution weighted towards larger clusters with well-delineated boundaries. In the special case of  $c_0 = 0.5, \beta = 1$  weak feedbacks lead to a “quench” sorting with clearly-delineated boundaries, albeit in a labyrinthine pattern (figure 4c-i). In some cases the low state extends along the  $\sigma$  axis as low cover is enforced by widespread feedbacks, such as when  $M > 1$  and in some cases where  $M = 1$  (figure 3a-1.0). As  $\beta$  increases with aspatial noise overwhelms weak local feedbacks and initial distribution of vegetation leading to neat-total overwhelming of initial conditions (figure 3b-0.4). Depending on external variability, then, the low state then exhibits convergence in (lack of) structure but divergence in cover.

The total area covered in the high state at high- $\sigma$ , high- $\phi$  is determined by the outside parameter  $M$  and the Gaussian kernel:  $M = 1$  converges on 0.5, while  $M = 0.4$  converges on 0.68 and  $M = 2$  on 0.32, approximating a normal distribution around each cell. So the high state is always associated with heterogeneous cover, displaying local structure universally across the landscape when the mortality ratio  $M \leq 1$  with little signal from initial conditions ( $U_{t-1}$  disperses and  $V_{t-1}$  diminishes the information transferred from  $S_{t-1}$ ). This local structure is found in both vegetated and gap spaces, leading to conditions under high  $\beta$  as in figure 3b-i where the high state’s cover is less than the low state’s. Additionally, under high  $\beta$  where  $M \leq 1$ , the areas along the  $\sigma$  axis take the high rather than the low state. Where  $M \geq 1$  power law likelihood is *reduced* by random mortality breaking networks of spatial organization even as extensive feedbacks allow overall cover to be maintained. Thus when crossing  $M = 1$  in the high state low state we see continued convergence on cover but divergence in structure.

In the parameter spaces between low and high state (intermediate  $\sigma$ , intermediate  $\phi$ ) power law organization exists in the handful of cells without complete spin-up at  $t = 500$ , indicating power law likelihood can be associated with transitions between states, even if neither the initial (random) and final states show little to no evidence of power law structure (figure a,b,c-2.0). following the expectation from a phase transition in a landscape, where the shift from one phase to another exhibits power-law scaling. In fig. 4a-iii, for instance, vegetation levels dropping towards a low states generates coarse-scale heterogeneity across the landscape as superclusters with higher initial density persist longer. The

margins and interiors of these superclusters are themselves heterogeneous as the vegetation clusters shrink in accordance with a power law distribution. Since there is no trend towards higher or lower land cover in figure 4c-iii there are similar areas of both uniform vegetation and uniform gap surrounded by power-law-structured vegetation and gap areas. These transitionary areas also have the highest coefficient of variation in total cover from seed to seed albeit still low, with  $CoV \approx 0.01$  at  $\beta = 1$ . Increasing  $\beta$  reduces the importance of distributions by increasing spatially unbiased inputs, resulting in more spatially uniform, locally heterogeneous new establishment, again pushing towards a global shift in state where initial spatial distribution has little influence.

The intermediate state at low  $\sigma$ , high  $\phi$  (ii. in figures 4,6) consistently exhibits stable power law structure regardless of overall cover in cases where  $M \geq 1$ . Rather than spreading fine-grained heterogeneity, at low  $\beta$  this area exhibits uniform structured heterogeneity across the landscape but without landscape-wide connectivity at low starting populations, and even in with higher landscape populations there is a lesser degree of global connectivity and an increase in near-adjacent clusters (compare the relatively reticulated patterns in figure 4c,i ii.). High  $\phi$  increases the importance of spatial interactions even as low  $\sigma$  keeps their extent tighter, resulting in noisier boundaries between vegetated areas than in the low state as random establishment is only retained by these strong-but-local spatial interactions At  $M = 1$  and low  $\beta$  this area is indistinguishable by landscape coverage or power law likelihood and is only apparent from spatial organization, visible both in the case of (figure 4a-ii., 4c-ii.). This results in long-term persistence of isolated-but-structured clusters even under long time spans, evidence this state truly is an alternate one, albeit only arising under stressed conditions ( $M \geq 1$ ). Even at high  $\beta$ , where there is a convergence in cover but still some difference in how each landscape approaches maximum cover, there remains some difference in organization of cell networks, with a median cluster size lower in under inextensive feedbacks case 4b-ii than under extensive ones case 4b-iv (25974 vs. 33081 cells, respectively).

After a mortality event is introduced, only  $M \leq 1$  exhibits any recovery past a universal low state. The low state remains at low cover, though at higher  $\beta$  there is some measure of spatially-facilitated recovery, leading to a higher  $p$ -value. At low values of  $\beta$  the high state is most resilient in cover, even as power law likelihood disappears as in the high mortality cases in figures 5,6. As  $\beta$  increases, though, strong and extensive feedbacks maintain gaps created in the mortality event and leave the area with low cover. The most resilient in *structure* remains in the intermediate state, where close ranges of strong facilitation lead to some residual survival and preferential nearby establishment in cover, which is also

evidenced by the distribution of cluster sizes visible in FIGURE. This effect is most pronounced in bases of higher  $\beta$  (figure 5b), where the intermediate state has the highest levels of cover relative to the rest of the parameter space. The appearance final states here are not dissimilar to those in under regular, non-hysteresis conditions (figure 6 a,c-i,ii), with those in the  $\beta = 5$  well on their way to recovery; given that  $M = 0.4$  in these examples such recovery is like to be towards a low-organization, but high cover, state as in figure 3a,b-i. While there remains greater cover than other cells of higher  $\sigma$ , in  $\beta = 5$  cover is at the high- $\sigma$ , high- $\phi$  corner is further attenuated, as connectivity between clusters is lost both at the scale of fine networks but also between large areas of the landscape (figure 6b-iv). This may be compared to the unstable states described in figure 4a-iii, where consistent intermediate-scale feedbacks lead to slow change towards the high or low state.

Based on this we can revise our conceptual model from figure 1 and add how it responds under disturbance (figure 7). Initial conditions and outside conditions are dominant in the low- $\sigma$ , low- $\phi$  corner, though it is worth emphasizing that both of these are still mediated through spatial feedbacks, only the transition to a final state exhibits spatial self-organization that manifests as a power law structure, consistent with a more classical phase transition. Transitions in cover at higher  $(\sigma, \phi)$  evolve not from discrete clusters growing but rather a mosaic of high and gap states that either spread or, in the cases of fig. 4a-iii, 4b-iii, eventually settle into one of the states; scale of process, not strength seems more important here (thus the revision in the high- $\sigma$ , low- $\phi$  corner in figure 7b). Cover in this high state is relatively stable under a wide variety of parameter spaces in the absence of a  $\phi$ , and the more heterogeneously-clustered intermediate cover exhibits stable organization even under high  $M$ , with or without a mortality event. While there is a relatively clear split in parameter space between high, low, and intermediate state, within each case there is little evidence of threshold behavior within the run of each case, consistent with some recent observations of landscape change supporting more gradual than catastrophic shifts over time (*Bhattachan et al.*, 2014). The resilience of power-law structure under a wide parameter space, especially in the intermediate state, is consistent with *Pascual and Guichard* (2005)'s robust criticality.

#### 4 Implications for process scale & inferring landscape change

Even weak and local stable process external climatic variability. When the overall trend in the landscape is more hostile to vegetation, this still results the sort of heterogeneous landscapes as in figure 4a-i. This non-power law distribution of cluster sizes is in accord with *Maestre and Escudero* (2009)'s

observation that semiarid landscapes in Spain do not exhibit scale-free relationships but are skewed towards larger cluster sizes which serve as facilitative sites for maintenance of vegetation. Under higher variability in death and establishment even the low-feedback area can exhibit some evidence of power law cluster size distributions while in transition, as in figure 4b-i, as clusters grow and are chained together, increasing the connectivity of feedback processes. It may be expected that cluster size distributions in landscapes with very localized, weaker feedbacks may approach and retreat from power law probabilities across growing cycles, with a large cluster-skewed frequency distribution of clusters remaining an attractor as larger clusters serve as loci of resilience.

The “uniform heterogeneity” in is largely a consequence of how the high-state can be considered a system with well-mixed disturbance. If we substitute “establishment” and “mortality” with “recovery” and “disturbance” we see a model fairly similar to the classic Ising-based models of forest disturbance pioneered by *Katori et al.* (1998) at  $M \leq 1$ , with the breaking of structure at  $M > 1$  consistent with the lack of a recovery phase in our landscape. A comparison can be made to widespread feedbacks, such as local recycling of moisture. The slow transition to one state or another in each discrete  $(\sigma, \phi)$  parameter space is consistent with the dynamics of landscapes sustained by large-scale feedbacks *without disturbance* (*Ahstrom et al.*, 2017). It is often under cases of *disturbance*—either natural as by fire or anthropogenic as with grazing—that abrupt boundaries appear between grass states and forest states still sustained in a well-mixed “high state” organized evaporation-precipitation feedbacks (*Oliveras and Malhi*, 2016). This is comparable to the relatively mosaic hard-edged mosaics in the cases of mortality or unstable spatial transitions, where larger-scale productivity is locally broken when interacting with another feedback-supported state; even though the unstable case in figure 4a-iii was not maintained over the long term, a constant disconnection and reconnection of feedback connectivity may have the effect of a constant instability, or true landscape-scale bistability.

The intermediate state in figures 4a-ii and 4c-ii is, like the high state, uniform, but the individual clusters lack the “uniform heterogeneity,” especially at low  $\beta$  instead consisting of solid core clusters as in the low state but with noisy, power-law distributed clusters adjacent and near-adjacent without landscape-wide connectivity. Ecohydrological feedbacks are considered the most likely candidates for such robust, relatively short-range (meters) feedbacks. In arid regions overlapping root systems a combination of root-facilitated soil water uptake, canopy shading of soil, canopy prevention of rainsplash soil compaction, as well as recycling of nutrients via leaf litter (*Caylor et al.*, 2006; *D'Odorico et al.*, 2005, 2007; *Scanlon et al.*, 2007; *Wainwright et al.*, 2009). The appearance of a state consisting of isolated

clusters stressed is also in accord with the such patterns occurring under conditions of water stress (figure 3, column 2.0), such as in with the decreasing area under facilitation roughly to the thresholds for facilitation seen in more process-based models (*Caylor et al.*, 2006; *D'Odorico et al.*, 2005).

After a mortality event and likewise can serve as connected networks for expansion back to a high state, as the similarity between strong recovery in the low  $\sigma$  parameter spaces across  $\phi$ , both in the high- $\beta$  and post-mortality case also demonstrate how such short-range feedbacks can chain into larger ones still exhibiting power law structure without long-range facilitation, consistent with the dense savannah landscapes under increasing moisture described by *Scanlon et al.* (2007). Recovery after a mortality event is likewise strong in this area of the parameter space both due to intrinsic parameters for facilitation and greater survival of facilitation networks (best observed in figures 5b, 6b-ii), but it is worth noting this depends on the the uniformity of our landscape's underlying conditions, with spatial facilitation and regrowth happening in much the same way as before the disturbance. In an actual mortality event the full hydro-ecogeomorphic system is may be disrupted, leading to changes in facts such as soil structure or nutrient supply. As such, after a mortality event resilient clusters may the distribution found in in figures 4a-i,6a-i (corresponding to cases where  $M > 1$  after a disturbance, when no recovery occurred).

An alternative mechanism—and one more applicable beyond arid environments—is the abilities of canopies to capture longwave radiation emitted at night. One of the clearest examples of a purely facilitative feedback is the role of radiative feedback. *He et al.* (2010) and *D'Odorico et al.* (2010)'s studies of microclimates in the northern Chihuahuan Desert compared grassland temperatures with those dominated by the shrub *Larrea tridentata*. While the mechanism for warming is under-canopy, the effect diffuses to a landscape scale of of  $\sim 100$  m. On average the shrub-dominated landscapes were  $2^\circ$  relative to nearby grasslands, with differences of  $8^\circ$  on the coldest nights, reducing winter freeze-induced mortality across the landscape. Similar facilitation processes—both in preventing mortality winter and enhancing summer growth—have been observed in boreal forests (*MacDonald et al.*, 2008). Empirical studies and models of alpine treelines have shown a similar dynamic, both in terms of preventing mortality and facilitating growth, with chains of weakly-connected clusters advancing northwards, again likely sustained by such radiative feedbacks (*Resler and Fonstad*, 2009; *Zeng and Malanson*, 2006) While the feedback processes in this model are isotropic, new establishment beyond northern or altitudinal margins of boreal and alpine landscapes produce similar, high power law likelihood patterns of establishment resembling the robustly critical cases in the intermediate state. Such feedbacks are

likely to occur on the scale of meters to tens of meters.

The above feedbacks highly specific, both in different scales of feedback (e.g. the radiative facilitation under mangroves, another cold-limited woody plant species currently expanding its range, are probably restricted to the immediate area around under-canopy spaces, pers. comm K. Cavanaugh and R. Bardou, 2018), so radiative feedback may be associated with the intermediate state or a transition to a high state. Additionally, the presence of a feedback process is dependent not just on plant species but the facilitative effects of the surrounding environment, e.g. for ecohydrological facilitation soil properties need to comport with infiltration and root system properties, for boreal and alpine facilitation the effectiveness of the above litter-microbial feedbacks to prime soil for future expansion. The capability for recovery these factors remaining constant, which is not necessarily the case in a large-scale mortality event. Additionally, there needs to be some base for recovery to continue, either from small surviving clusters or new establishment creating new clusters for recovery.

## 5 Conclusion

We establish a model that reproduces heterogeneous landscapes based on a combination of local feedbacks and global tendency towards change, many of which exhibited power-law scaling laws in their distribution of cluster size. This was done without some of the common assumptions made in studies of landscape heterogeneity, such as the presence of separate facilitative and competitive processes or zones of interaction. Furthermore, in addition to generating clearly distinct landscape states at high and low levels of cover we also, by using the nonparametric power law test from (*Clauset et al.*, 2009) we found thresholds across our extent, scale ( $\sigma, \phi$ ) parameter space. Furthermore, this model reproduced different scales of and structures of heterogeneity in agreement with different environmental types: both unstructured and structured (not exhibiting and exhibiting power laws) observations in semi-arid to arid environments and structured, but high-cover examples in forested woody landscapes.

### UNRELIABILITY, ONLY IN LANDSCAPE SHIFT

This has implications for long-standing assumptions on the applicability of power law relations in landscapes. Heterogeneity is not evidence in itself of incipient change, although it is always associated with shifts in landscape (see the emergence of power laws in figure 3b-0.4, 4b-i., 5b-0.4, 6b-i.), in accordance with classical models of state change. These final states can still exhibit stable heterogeneity, resulting in a “quenched” state typically with hard boundaries between states depending on the starting population and a rank-order distribution weighted towards larger (relative to overall cluster area)

clusters; such states . Power-law structure can be maintained, though, either in the presence of strong long-range feedbacks, maintaining power-law structure over long areas as external variability is mixed into the structure, making for a uniformly self-organized structure.

The presence of long-lived spatial heterogeneity in stressed (equal or higher ratios of mortality to establishment) imply the presence of short-range, sustaining feedbacks. The observations of such distributions of woody plants in arid and semi-arid and arid landscapes over long periods of time suggests dynamics akin to *Pascual and Guichard* (2005)'s concept of robust criticality. Yet, given the presence of similar dynamics during transition, even under weak feedback strength, there remains some ambiguity. As such, power law relationships are not enough to discern the state or direction of a landscape—they are not necessarily associated with stable heterogeneity they can represent change or stability, and long-term resilience of cover can still occur in their absence. While evidence of spatial self-organization can provide insights into the processes shaping landscapes and their *potential* dynamics, they must be put in the context of other studies of landscape history and geo-ecological process.

Additionally, this model started with random initial distributions of vegetated cells and, while spatial feedbacks influenced the establishment or mortality of interannual noise to the landscape, the noise inputs themselves were likely aspatial. While such processes can occur on the landscape scale, such as landscape-scale interannual variability in precipitation or temperature, but while event-based changes are important for understanding landscape structure and resilience at centennial or shorter timescales longer-term changes require, in the terms of this study, a shift in  $M$ , and given increasing global favorability towards woody plants a shift from  $M = 1$  to  $M < 1$ . With constant mortality ratios stressed, intermediate-state environments will either spread into either high-cover, low-structure state or a high state with well-mixed power law structure without catastrophic shift in state over time. Furthermore, while spread in this model would be even across the landscape, in real landscapes they would be associated with landscape features facilitating longer within-landscape connectivity (e.g. preferential corridors for water, nutrient, or propagule transport) or expansion along a gradient, such as expansion of the “fuzzy” edge of a treeline northward with increasing temperatures.

Similarly, disruption often takes a spatially heterogeneous form beyond the uniformly-forced mortality in this model. Such disruption, when well-mixed across a landscape, simply breaks structure and reduces cover, with the lack of any explicit recovery mechanism (typical in such models; *Katori et al.* 1998; *Pascual and Guichard* 2005) in the face of high external mortality breaking structure. Strong breaks in structure during mortality events lead to the emergence of hard-edged borders between gap

spaces (FIGURE), much as in the high state-gap mosaics that temporarily occur in cases without external disturbance (FIGURE; in FIGURE there are also hard edges between uniformly vegetated areas due to equal starting ratios of vegetation to gap). Depending on their location on the parameter space such shifts could lead to an abrupt shift. However, given the overall similarity between each surface this zone is likely small unless coupled with some change in interannual variability either promoting or preventing new establishment.

While large-term external variability across the  $M$  parameter may be a consequence of change in time, *within* each  $(\sigma, \phi)$ , such as year-to-year changes in connectivity of feedback processes due to such factors as shifting levels of ecological competition or changing disturbance-recovery patterns over time, provide potential explanation for landscape heterogeneity between small clusters and large-scale organized stability. Without even forcing or a single discrete mortality event, though, the scale of interaction—and thus level of connectivity—can change dynamically over time, leading to shifting mosaics at the borders of landscape types, such as those observed on the borders between forest and savanna landscapes (*Oliveras and Malhi, 2016*). Such localized disturbance, between the level of close-scale patterns in vegetation clusters and landscape-scale structure, provide a fruitful avenue of study both in modeling how such disturbance stabilizes mosaics and responses from either short- or long-range self-organization.

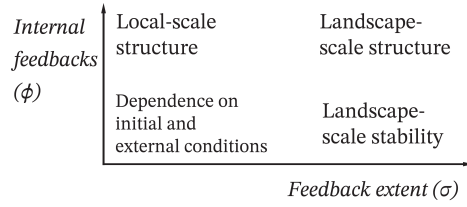


Figure 1: We expect the following dynamics after running the model at varying feedback extents ( $\sigma$ ) and strengths ( $\phi$ ). At low values of both initial conditions are expected to persist, or changes due to external forcings will be purely dependent on them. In the opposite high- $\sigma$ , high- $\phi$  quadrant we expect landscapes to exhibit widespread self-organized structure (with *structure* defined as exhibiting a power-law size distribution.) as internal feedbacks are dominant. At high- $\sigma$ , low- $\phi$  we expect landscape-wide stability without organization as they are stabilized by long-range feedbacks without strong enough short-range facilitation to lead to structure, and short-range structure without landscape-level effects in the opposite low- $\sigma$ , high- $\phi$  corner.

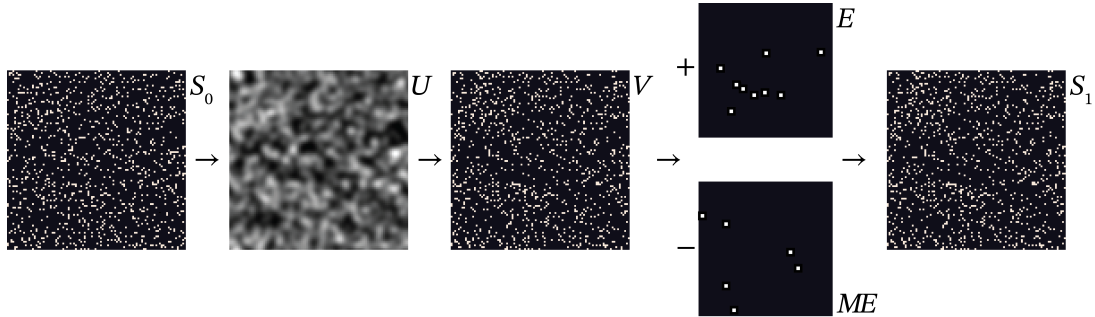


Figure 2: Diagram of model progression over each timestep: moving from  $S_0$  to  $U$  we Gaussian blur the initial state grid at a variance  $\sigma$ . The probability that any given site  $x$  on  $V$  will be occupied is given by  $\phi U_x + (1 - \phi)S_x$ , resolving into values of 0 or 1. Grids randomly generated for establishment  $E$  and mortality  $ME$  (with cells magnified here for demonstration) are then added and subtracted, yielding  $S_1$ . Landscapes depicted are 1% as large as landscapes used in model.

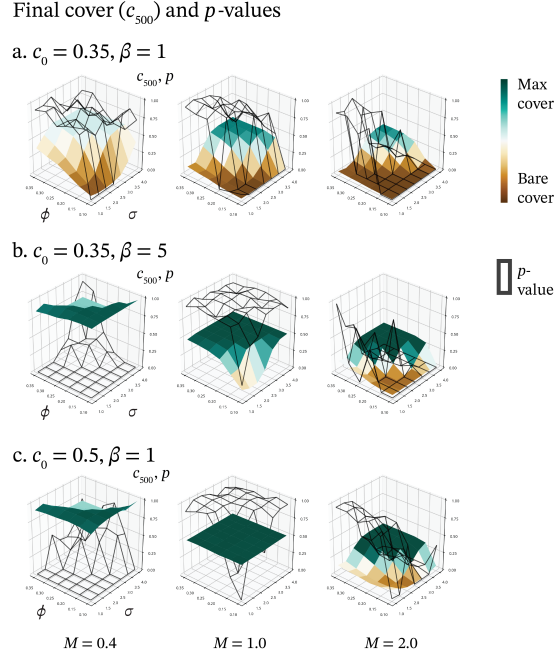


Figure 3: Land cover  $c_{500}$  and power law probability  $p$  for each  $(\sigma, \phi)$  space, with each  $(\sigma, \phi)$  surface arranged according to mortality/establishment ratio  $M$  and rows based on initial starting population  $c_0$  and outside variability  $\beta$ ; row numbering is consistent across figures (e.g. row a. always describes  $c_0 = 0.35, \beta = 1$  in figure 4 as well);  $c_0 = 0.5, \beta = 5$  is excluded since it has similar cover dynamics as  $c_0 = 0.5, \beta = 5$  and the effects of increasing  $\beta$  on cluster morphology are similar to  $c_0 = 0.35, \beta = 5$  (figure 5). Since cover in the “high” state is regulated by the overall mortality ratio, the colorbars indicating state are scaled by mortality ratio, not absolute levels of cover. The wireframe surface represents power law probability  $p$ . Note the special case at  $M = 1, c_0 = 0.5, \beta = 1$  where cover is uniform across the  $(\sigma, \phi)$  surface but power law probability varies.

Final cover maps at  $M = 1$

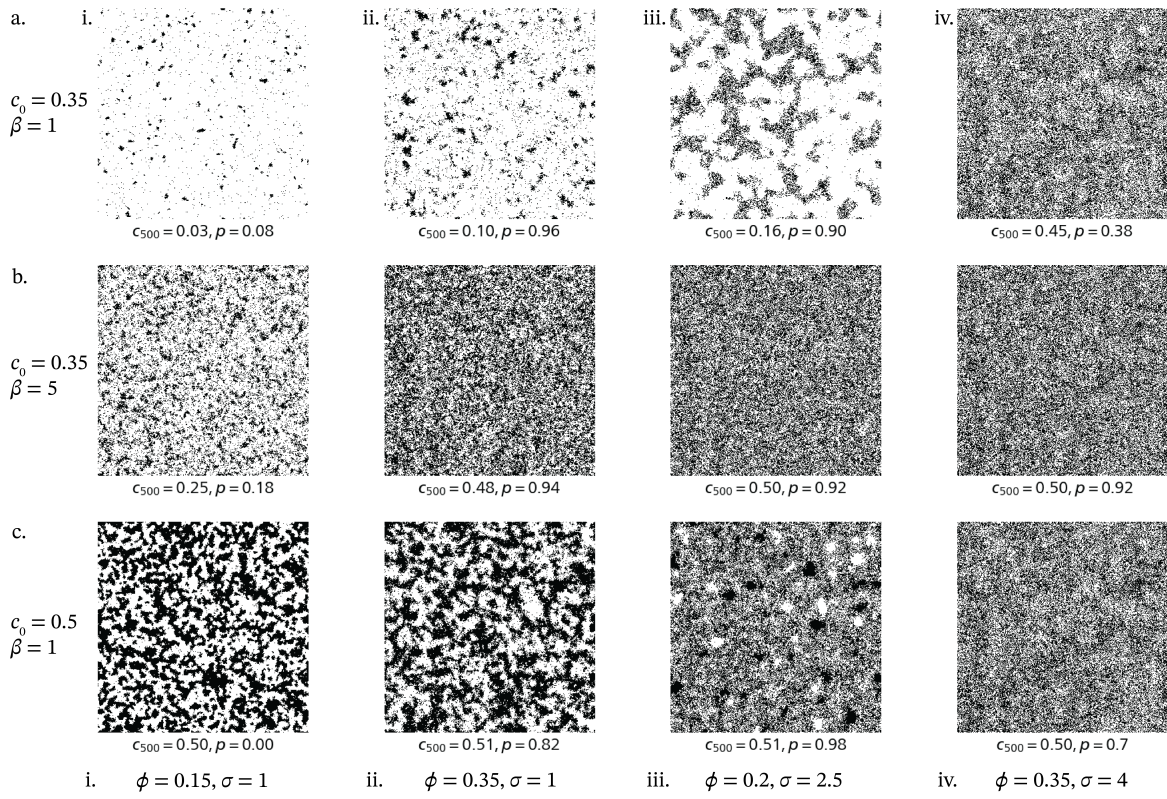


Figure 4: Examples of land cover  $c_{500}$  at  $M = 1$  Column i. is the low state at minimal  $(\sigma, \phi)$ . ii. is the intermediate state and minimal  $\sigma$ , maximal  $\phi$ , iii. an unstable at  $t = 500$  state at  $(\sigma, \phi) = 2.5, 0.2$ , declining to the low state in row a., increasing to the high state in row b, and in a steady state of cover row c., and column iv. is the high state at maximal  $(\sigma, \phi)$

Post-mortality event ( $M = 8$ ),  
recovery at  $M = 0.4$

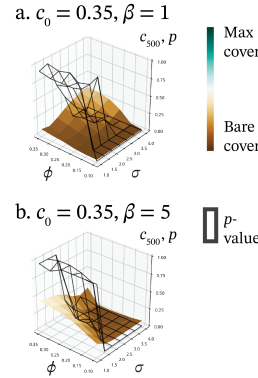


Figure 5:  $(\sigma, \phi)$  surfaces for land cover  $c_{500}$  after a mortality event at  $M = 8$  and a recovery condition of  $M = 0.4$  for greater clarity of recovery dynamics; similar dynamics are seen at  $M = 1$  and  $c_0 = 0.5$  and are excluded for conciseness, as are cases when  $M > 1$  as they exhibit zero recovery after the mortality event.

Final cover maps at high-growth  $M = 0.4$  after disturbance event ( $M_{\text{dist}} = 8$ )

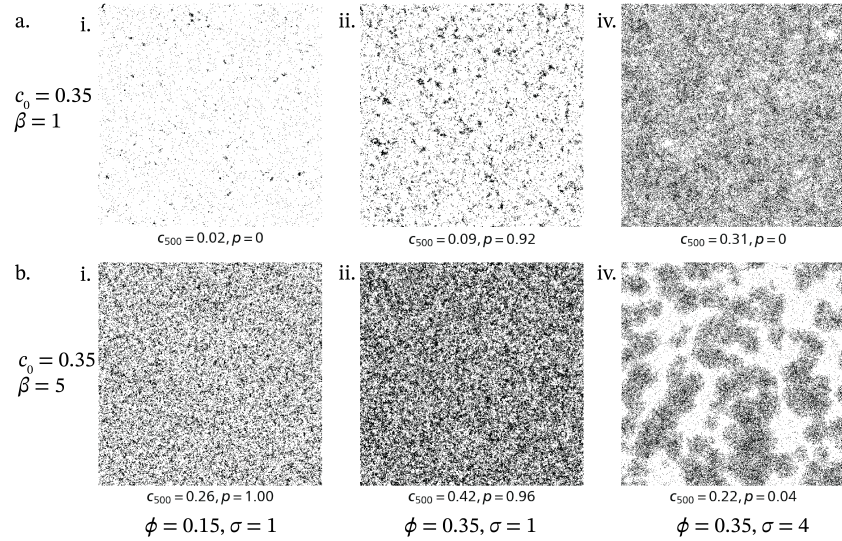


Figure 6: Examples of recovering land cover  $c_{500}$  on the  $(\sigma, \phi)$  surface after a mortality event at  $M = 8$  and a recovery condition of  $M = 0.4$  for greater clarity of recovery dynamics. Examples from the middle of the surface  $((\sigma, \phi) = 0.25, 2.0)$  are less relevant so column iii. is excluded.

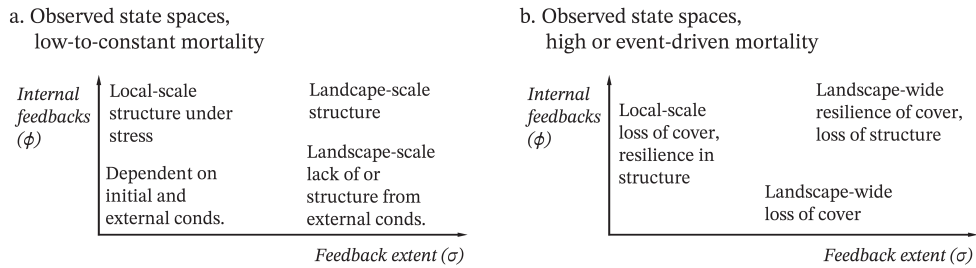


Figure 7: Revising the expected change space in figure 1, in diagram a. we find a broad similarity with expectations from figure 1 with some revisions. Only the minimal and maximal corners in  $(\sigma, \phi)$  space consistently manifest. The high  $\sigma$ , low  $\phi$  corner can take on the characteristics of either the minimal or maximal corner depending on starting population and outside conditions, with a greater tendency toward the unstructured state. The low- $\sigma$ , high- $\phi$  corner only manifests a distinct set of local-scale dynamics under stress, but converging towards the unstructured state when  $M < 1$  (figure 3). Under greater stress or after a mortality event the dynamics in structure and cover are often reversed, with some cover remaining at the maximal  $(\sigma, \phi)$  corner without structure but stronger resilience or growth of locally self-organized cells in the higher- $\phi$  area, which lead the recovery of the landscape (figure 5)

## References

- Ahstrom, A., J. G. Canadell, G. Schurgers, M. Wu, J. A. Berry, K. Guan, and R. B. Jackson, Hydrologic resilience and Amazon productivity, *Nature Communications*, 8(387), 2017.
- Alstott, J., E. Bullmore, and D. Plenz, Powerlaw: A Python package for analysis of heavy-tailed distributions, *PLoS One*, 9(1), e85,777, 2014.
- Bak, P., C. Tang, and K. Wiesenfeld, Self-organized criticality: An explanation of 1/f noise, *Physical Review Letters*, 59(4), 381–384, doi:10.1103/PhysRevLett.59.381, 1987.
- Bhattachan, A., P. D'Odorico, K. Dintwe, G. Okin, and S. Collins, Resilience and recovery potential of duneland vegetation in the southern Kalahari, *Ecosphere*, 5(1), 2, doi:10.1890/ES13-00268, 2014.
- Caylor, K., P. D'Odorico, and I. Rodriguez-Iturbe, On the ecohydrology of structurally heterogeneous semiarid landscapes, *Water Resources Research*, 42, W072,424, doi:doi:10.1029/2005WR004683, 2006.
- Clauset, A., C. R. Shalizi, and M. E. J. Newman, Power-law distributions in empirical data, *SIAM Review*, 51(4), 661–703, doi:10.1137/070710111, 2009.
- D'Odorico, P., F. Laio, and L. Ridolfi, Noise-induced stability in dryland plant ecosystems, *Proceedings of the National Academy of Sciences*, 102(31), 10,819–10,822, doi:10.1073/pnas.0502884102, 2005.
- D'Odorico, P., F. Laio, and L. Ridolfi, Vegetation patterns induced by random climate fluctuations, *Geophysical Research Letters*, 33, L19,404, doi:10.1029/2006GL027499, 2006.
- D'Odorico, P., K. Caylor, G. S. Okin, and T. M. Scanlon, On soil moisture–vegetation feedbacks and their possible effects on the dynamics of dryland ecosystems, *Journal of Geophysical Research*, 112, G04,010, doi:10.1029/2006JG000379, 2007.
- D'Odorico, P., J. Fuentes, W. Pockman, S. Collins, Y. He, J. Medeiros, S. DeWekker, and M. Litvak, Positive feedback between microclimate and shrub encroachment in the northern chihuahuan desert, *Ecosphere*, 1(6), art17, doi:10.1890/ES10-00073.1, 2010.
- D'Odorico, P., A. Bhattachan, K. Davis, S. Ravi, and C. Runyan, Global desertification: Drivers and feedbacks, *Advances in Water Resources*, 51(January 2013), 326–344, doi:10.1016/j.advwatres.2012.01.013, 2013a.
- D'Odorico, P., Y. He, S. Collins, S. F. J. D. Wekker, V. Engel, and J. D. Fuentes, Vegetation–microclimate feedbacks in woodland–grassland ecotones, *Global Ecology & Biogeography*, 22, 364–379, doi:10.1111/geb.12000, 2013b.

- Götmark, F., E. Götmark, and A. M. Jensen, Why be a shrub? A basic model and hypotheses for the adaptive values of a common growth form, *Frontiers in Plant Science*, 7, 1095, doi:10.3389/fpls.2016.01095, 2016.
- He, Y., P. D'Odorico, S. F. J. de Wekker, and J. D. Fuentes, On the impact of shrub encroachment on microclimate conditions in the northern chihuahuan desert, *Journal of Geophysical Research*, 115, D21,120, doi:10.1029/2009JD013529, 2010.
- Holling, C., Resilience and stability of ecological systems, *Annual Review of Ecology & Systematics*, 4, 1–23, doi:10.1146/annurev.es.04.110173.000245, 1973.
- Katori, M., S. Kizaki, Y. Terui, and T. Kubo, Forest dynamics with canopy gap expansion and stochastic ising model, *Fractals*, 6(1), 81–86, doi:10.1142/S0218348X98000092, 1998.
- Kéfi, S., M. Rietkerk, C. L. Alados, Y. Pueyo, V. P. Papanastasis, A. ElAich, and P. C. de Ruiter, Spatial vegetation patterns and imminent desertification in Mediterranean arid ecosystems, *Nature*, 449(13 September), doi:10.1038/nature06111, 2007.
- Lefever, R., and O. Lejeune, On the origin of tiger bush, *Bulletin of Mathematical Biology*, 59(2), 262–294, doi:10.1016/S0092-8240(96)00072-9, 1997.
- Lejeune, O., P. Couteron, and R. Lefever, Short range co-operativity competing with long range inhibition explains vegetation patterns, *Acta Oecologica*, 20(3), 171–183, doi:10.2307/3237141, 1999.
- MacDonald, G., K. Kremenetski, and D. Beilman, Climate change and the northern Russian treeline zone, *Philosophical Transactions of the Royal Society B*, 363, 2285–2299, doi:10.1098/rstb.2007.2200, 2008.
- Maestre, F. T., and A. Escudero, Is the patch size distribution of vegetation a suitable indicator of desertification processes?, *Ecology*, 90(7), 1729–1735, doi:10.1890/08-2096.1, 2009.
- Moreno-de las Heras, M., P. M. Saco, G. R. Willgoose, and D. J. Tongway, Assessing landscape structure and pattern fragmentation in semiarid ecosystems using patch-size distributions, *Ecological Applications*, 21(7), 2793–2805, 2011.
- Noy-Meir, I., Stability of grazing systems: An application of predator-prey graphs, *Journal of Ecology*, 62(2), 459–481, doi:10.1080/00107510500052444, 1975.
- Okin, G. S., P. D'Odorico, and S. R. Archer, Impact of feedbacks on chihuahuan desert grasslands: Transience and metastability, *Journal of Geophysical Research*, 114, G01,004, doi:10.1029/2008JG000833, 2009.
- Oliveras, I., and Y. Malhi, Many shades of green: the dynamic tropical forest-savannah transition zones,

- Philisophical Transactions of the Royal Society B*, p. 20150308, doi:10.1098/rstb.2015.0308, 2016.
- Pascual, M., and F. Guichard, Criticality and disturbance in spatial ecological systems, *Trends in Ecology & Evolution*, 20(2), 88–95, doi:10.1016/j.tree.2004.11.012, 2005.
- Resler, L. M., and M. A. Fonstad, A markov analysis of tree islands at alpine treeline, in *The Changing Alpine Treeline*, edited by D. R. Butler, G. P. Malanson, S. J. Walsh, and D. B. Fagre, pp. 151–166, Elsevier, Amsterdam, 2009.
- Rietkerk, M., S. C. Dekker, P. C. de Ruiter, and J. van de Koppel, Self-organized patchiness and catastrophic shifts in ecosystems, *Science*, 305, 1926–29, doi:10.1126/science.1101867, 2004.
- Runyan, C. W., P. D'Odorico, and D. Lawrence, Physical & biological feedbacks of deforestation, *Reviews of Geophysics*, 50, RG4–6, doi:10.1029/2012RG000394, 2012.
- Sankaran, M., J. Ratnam, and N. Hanan, Tree–grass coexistence in savannas revisited – insights from an examination of assumptions and mechanisms invoked in existing models, *Ecology Letters*, 7, 480–490, doi:10.1111/j.1461-0248.2004.00596.x, 2004.
- Scanlon, T. M., K. K. Taylor, S. A. Levin, and I. Rodriguez-Iturbe, Positive feedbacks promote power-law clustering of Kalahari vegetation, *Nature*, 449(13 September), 209–213, doi:10.1038/nature06060, 2007.
- Solé, R. V., and S. C. Manrubia, Are rainforests self-organized in a critical state?, *Journal of Theoretical Biology*, 173, 31–40, doi:10.1006/jtbi.1995.0040, 1995.
- Stewart, J., A. J. Parsons, J. Wainwright, G. S. Okin, B. T. Bestelmeyer, E. L. Fredrickson, and W. H. Schlesinger, Modeling emergent patterns of dynamic desert ecosystems, *Ecological Monographs*, 84(3), 373–410, doi:10.1890/12-1253.1, 2014.
- Virkar, Y., and A. Clauset, Power-law distributions in binned empirical data, *Annals of Applied Statistics*, 8(1), 89–119, doi:10.1214/13-AOAS710, 2014.
- Vuong, Q., Likelihood ratio tests for model selection and non-nested hypotheses, *Econometrica*, 57(2), 307–333, doi:10.2307/1912557, 1989.
- Wainwright, J., A. J. Parsons, E. N. Müller, R. E. Brazier, and D. M. Powell, Response to Hairsine's and Sander's "Comment on "A transport-distance based approach to scaling erosionrates: Parts 1, 2 and 3 by Wainwright et al." , *Earth Surface Processes & Landforms*, 34, 886–890, doi:10.1002/esp.1781, 2009.
- Wang, L., P. D'Odorico, J. Evans, D. Eldridge, M. McCabe, K. Taylor, and E. King, Dryland ecohydrology and climate change: critical issues and technical advances, *Hydrology & Earth System Sciences*, 16, 2585–2603, doi:10.5194/hess-16-2585-2012, 2012.

Westoby, M., B. Walker, and I. Noy-Meir, Opportunistic management for rangelands not at equilibrium, *Journal of Range Management*, 42(4), 266–274, 1989.

Yizhaq, H., Y. Ashkenazy, , and H. Tsoar, Why do active and stabilized dunes coexist under the same climatic conditions?, *Physical Review Letters*, 98(4 May), 188,001, doi:10.1103/PhysRevLett. 98.188001, 2007.

Zeng, Y., and G. P. Malanson, Endogenous Fractal Dynamics at Alpine Treeline Ecotones, *Geographical Analysis*, 38, 271–287, doi:10.1111/j.1538-4632.2006.00686.x, 2006.